Proceedings of the ASME 2017 36th International Conference on Ocean, Offshore and Arctic Engineering
OMAE2017
June 25-30, 2017, Trondheim, Norway

OMAE2017-61779

EFFECT OF THE BEAM ELEMENT GEOMETRIC FORMULATION ON THE WIND TURBINE PERFORMANCE AND STRUCTURAL DYNAMICS

Virgile Delhaye*
SINTEF Ocean[1]
Trondheim, Norway

Madjid Karimirad**
SINTEF Ocean[1]
Trondheim, Norway

Petter Andreas Berthelsen
SINTEF Ocean[1]
Trondheim, Norway

ABSTRACT

In this paper, the original double symmetric cross section beam formulation in RIFLEX used to model the blades is compared against a newly implemented generalised beam formulation, allowing for eccentric mass, shear and elastic centres. The generalised beam formulation is first evaluated against an equivalent ABAQUS beam model (Using the generalised beam formulation implemented in ABAQUS) which consists of DTU 10MW RWT (reference wind turbine) blade in static conditions. A static displacement is applied to the tip, which is close to an operating load. The results appear very similar and ensure that the implementation is correct.

The extended beam formulation is afterwards used on the Land-based 10MW turbine from DTU with external controller. This case study aims at evaluating the effect of the newly implemented formulation on realistic, flexible structure. During the study, the blades were discretised using both the old and new formulation, and dynamic simulations were performed. The effect of the beam formulation was evaluated using several wind conditions that are thought to be characteristic of operating conditions. Results show slight difference between two formulations but could be more significant for next generation flexible blades.

---

* corresponding author. virgile.delhaye@sintef.no

**Current affiliation : Queen's University Belfast (QUB), United Kingdom (UK)

[1] Earlier MARINTEK, SINTEF Ocean from 1st January 2017 through a merger internally in the SINTEF Group

INTRODUCTION

There is a need to improve the structural predictions of the blade in aerodynamic codes without compromising with code's efficiency. This comes from the increased complexity and size of the new blade designs. In particular, improving the aerodynamic performances of the blade by tailoring the fibre reinforced plastic layers is an important research topic (Kooijman (1996) [1]). In this context, the use of advanced beam model able to better predict blade dynamics and give a more realistic description of the load transfer into the wind turbine becomes crucial for industry. A significant contribution in this field comes from helicopter technology and was developed by Hodges et al. (1999) [2], Yu et al. (2002) [3]. The idea is to reduce a three-dimensional anisotropic elastic problem to a two-dimensional cross section analysis and to a one-dimensional beam analysis (e.g. the variational asymptotic methodology by Berdichevsky (1979) [4]). These methodologies have been used to successfully describe the structural behaviour of single blade submitted to static and dynamic loadings (Otero (2010) [5]). The inclusion of such formulation in multibody codes, which are able to handle a whole wind turbine, is less common.

An anisotropic beam formulation was recently implemented in the multibody aeroelastic code HAWC2 (Branner et al., 2012 [6], Kim et al., 2013 [7]), in order to simulate full wind turbine structure and to capture the bend-twist effect arising in the next-gen blades as observed by Lobitz et al. (2000) [8] (2003) [9]. In the present paper, a similar step is presented in RIFLEX with the implementation of a generalised cross-section formulation to discretize the blades.

RIFLEX (MARINTEK, 2015 [10, 11]) is a computer program system developed by MARINTEK for analysis of slender marine structures. RIFLEX is a non-linear Finite Element (FE) solver that can perform coupled analysis of one or more rigid-body floating structures. It can include dynamic modelling of the mooring and riser systems and full coupling of forces in the time domain. The method is described by (Ormberg, Fylling, Larsen, & Sødahl, 1997 [13]), and verified by comparisons with model test results; see e.g. (Kendon et al., 2008 [14]; Ormberg, Stansberg, Yttervik, & Kleiven, 1999 [15]; Stansberg, Yttervik, Øritsland, & Kleiven, 2000 [16]; Stansberg, Øritsland, & Kleiven, 2000 [17]).

This paper focuses first on the load distribution along a straight blade in static conditions providing a preliminary benchmark test between the RIFLEX generalised beam implementation and the ABAQUS equivalent general beam section. Next, the effect of the beam formulation of the blade on the structural response of the wind turbine (Both globally and locally) is examined in constant wind with constant rotational speed. Afterwards, the effect of the beam formulation on the structural response in more complex inflow with constant rotor speed is also examined in order to highlight the effects of different engineering corrections. Finally, results in turbulent wind conditions are also presented in the paper. The details of the load magnitude are important for computing blade responses, and for further design checks such as fatigue and extreme load calculations.

DTU 10MW REFERENCE WIND TURBINE

The DTU 10 MW Reference Wind Turbine is a three-bladed, upwind tower and rotor with variable speed, collective pitch control (Bak et al., 2014 [18]). The overall characteristics of the structure are given in Table 1 and the model is illustrated Figure 1.

Table 1 : DTU 10 MW wind turbine principal characteristics.

Hub-height	119.0 m
Rotor diameter	178.3 m
Rotor mass	228 tonnes
Nacelle mass	446 tonnes
Tower mass	628 tonnes
Rated wind speed	11.4 m/s
Rated power	10 MW

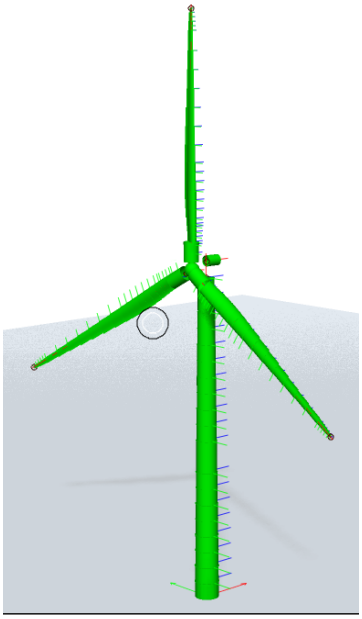

Figure 1: Illustration of the SIMA DTU 10MW land-based wind turbine.

Wind loads

The wind loads on the blades are computed based on the load coefficient description in the airfoil library file and together with a blade element momentum (BEM) method [10]. (BEM) method is an efficient way to determine the aerodynamic loading on wind turbine blades (Burton et al., 2011 [19]; Hansen et al., 2006 [20]; Manwell, McGowan, & Rogers, 2009 [21]).

The RIFLEX computer program has been extended to include aerodynamic forces on elastic structural members using blade element momentum theory (BEM) with a number of correction factors applied, including the Glauert correction, Prandtl tip loss factor, dynamic wake, dynamic stall, skewed inflow, and tower shadow (influence) [10,11]. In addition to the aerodynamic loads, the control system for blade pitch and electrical torque for power extraction can be modelled. The variable-speed generator torque and proportional-integral (PI) collective blade-pitch controllers use the feedback of the generator speed. At below-rated wind speeds, the controller only modifies the generator torque; at over-rated wind speeds, the control is active by feathering the blades.

The main features of the BEM theory implemented in RIFLEX are (Ormberg et al. (2011) [12]):

- Induced velocity is calculated assuming momentum balance for a ring-shaped control volume.
- Blade sections are treated as independent.
- Aerodynamic coefficients from wind tunnel tests are used for the blades.

- Empirical corrections are used for tip-vortices and cascade effects / lift amplification.
- the complete blade motions including the elastic twist are taken into account in the aerodynamic model

Control System

The definition of the DTU 10 MW RWT includes a description of the collective blade pitch and generator torque controller (Bak et al., 2014 [18]). The generator speed is used as feedback and a low-pass filtered wind speed is used to control the minimum blade pitch at below-rated wind speeds. This controller has been implemented as an external Java library which communicates with RIFLEX.

BLADES STRUCTURAL MODEL

Blade properties

As shown in Figure 2, the blade is discretized into 26 elements. The chord, blade profile (thickness), and twist are assumed constant over each element.

Two geometries are provided for the DTU 10 MW RWT blade: a straight geometry as well as a pre-bent configuration (3.332 m) (Bak et al., 2014 [18]). In the present paper, the pre-bent configuration (with offsets as in the first subplot of Figure 2) is used for the final elastic simulations.

Finally, the last subplot of Figure 2 shows the blade twist as constructed. The twist profile is only applied for the pre-bent blade.

The airfoils are thick airfoils based on the FFA-W3 series. For each element, airfoil data based on the interpolated value of the thickness at the center of the element must be created. The resulting lift coefficient (C_L) at several thicknesses is shown as a function of the angle of attack (α) in Figure 3. The provided lift coefficient data for the airfoils with 60 % and 48 % thickness includes some "kinks." The severe kink in the airfoil with 60 % thickness, which gives negative lift for some small positive values of the angle of attack, significantly affects the inboard profiles out to approximately 21 m.

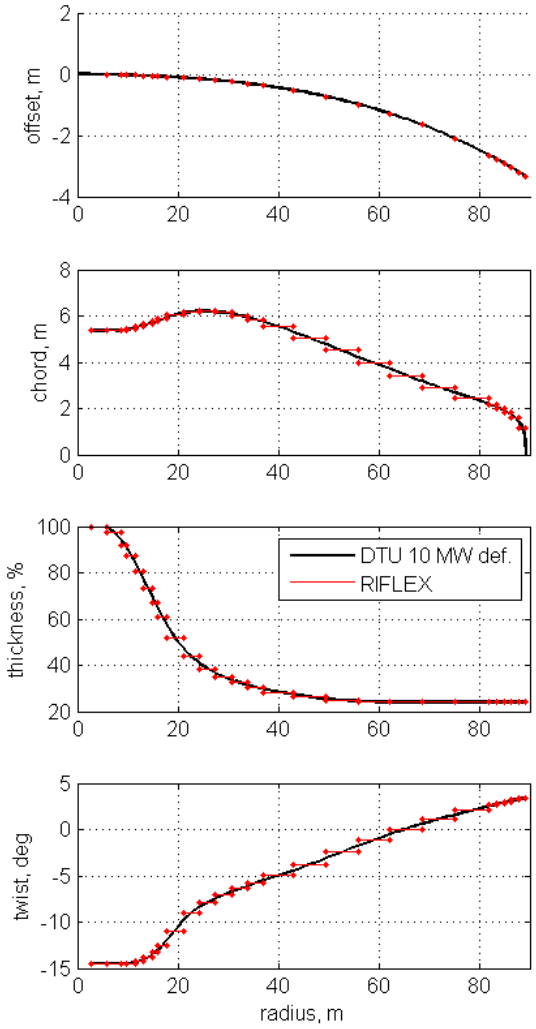

Figure 2 : DTU 10 MW blade properties as a function of radial distance from the hub.

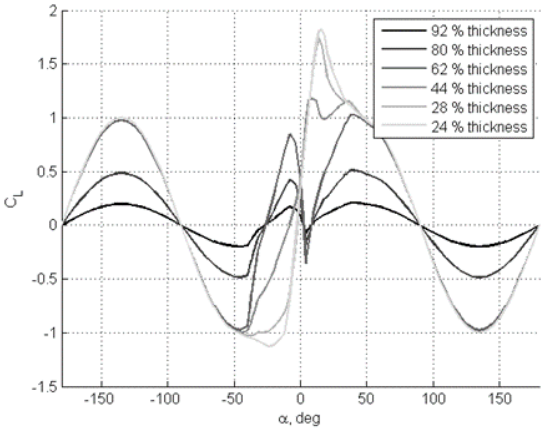

Figure 3 : Interpolated lift coefficients for selected blade section thicknesses.

Co-rotational beam formulation

The beam elements used to discretize the blade in RIFLEX have a co-rotational formulation. The basic idea in the co-rotational approach is to decompose the motion of the element into pure rigid body and pure deformation parts through the use of a reference frame that continuously rotates and translates with the element. The deformation is captured at the level of the co-rotated reference, while the geometric nonlinearity of the arbitrarily large rigid body motion is incorporated in the local-global transformation matrices. By assuming small deformations relative to the co-rotated element frames, linear elements can be re-used in a geometrically nonlinear context, which in fact is the main motivation for using co-rotational formulations (Battini, 2006 [23]; Felippa, 2005 [24]).

The co-rotational concept is illustrated in Figure 4 where the initial configuration of the element is denoted C_0, the co-rotated element configuration is labelled C_{0n} and the deformed configuration is denoted C_n. All stress and strain variables are referred to the straight C_{0n}-reference which differs from the initial C_0-configuration by the element rigid body motion. The co-rotational formulation can therefore be regarded as computationally equivalent to the total Lagrange formulation; however, issues such as membrane locking and artificial straining are avoided since the eliminated rigid body motion enables use of low-order strain measures (Mathisen, 1990 [25]).

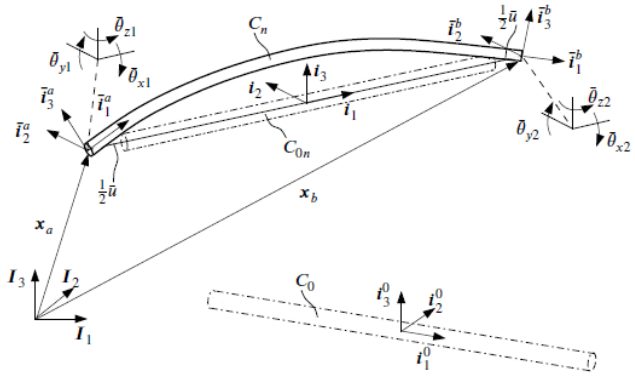

Figure 4 : Co-rotational beam element.

A standard co-rotational beam formulation is implemented in RIFLEX where the deformational parameters in Figure 4 are organized in the deformational displacement vector as follows,

$$\bar{v}_d = \left[-\frac{1}{2}\bar{u}\ \ 0\ \ 0\ \ \bar{\theta}_{x1}\ \ \bar{\theta}_{y1}\ \ \bar{\theta}_{z1}\ \ \frac{1}{2}\bar{u}\ \ 0\ \ 0\ \ \bar{\theta}_{x2}\ \ \bar{\theta}_{y2}\ \ \bar{\theta}_{z2}\right]^T \qquad (1)$$

where the bar symbol underlines that the deformational parameters refer to the element coordinate system and the beam element x-axis which intersects node a and b in Figure 4. The axial elongation $\bar{u}$ is computed as the difference between the current secant length between the element nodes and the initial length, while the rotational deformation parameters $\bar{\theta}_{x1}, \bar{\theta}_{y1}, \bar{\theta}_{z1}$, and $\bar{\theta}_{x2}, \bar{\theta}_{y2}, \bar{\theta}_{z2}$ are computed from the rotation tensor expressing the relative rotation from the element base vectors $\boldsymbol{i}_k$ to the nodal base vectors $\bar{\boldsymbol{\imath}}_{\boldsymbol{k}}$, see Figure 4. Further details about these computations are given in the RIFLEX 4.9.0 Theory Manual [10].

The internal load vector for a standard element with linear-elastic material properties is calculated from the relation,

$$\boldsymbol{S} = \boldsymbol{k}\bar{\boldsymbol{v}}_{\boldsymbol{d}} \qquad (2)$$

where $\boldsymbol{k}$ is the material stiffness matrix referred to the principal axes of a cross-section without offset shear and area centres relative to the beam axial reference line.

General cross section formulation

The constitutive response of general cross-sections is expressed in the principal axes coordinates to allow for direct use of the shear stiffness model in (Bell, 1987 [26]).

The principal axes V and W for the second area moment are formally determined by the requirement $\int_A VW dA = 0$ where A is the cross-section area. The angle of the principal V -axis measured relative to the beam element Y -axis is denoted θ, see Figure 5.

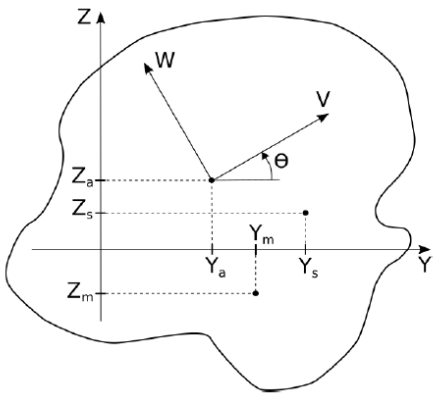

Figure 5 : General cross-section

Calibration of the general cross section type

For general cross-section, the mass centre (Y_m,Z_m), area centre (Y_a,Z_a) and shear centres (Y_s,Z_s) must be given in addition of the aerodynamic coordinate system and centre, see in Figure 6. Each of them is expressed in the blade coordinate system and origin which coincides with the elastic (local) (X_L;Y_L;Z_L) coordinate system ([10]) and the beam coordinate system (Y,Z) from Figure 5 .

For airfoil elements that are part of a wind turbine blade the local X_L-axis is pointing towards the blade tip for upwind conditions.

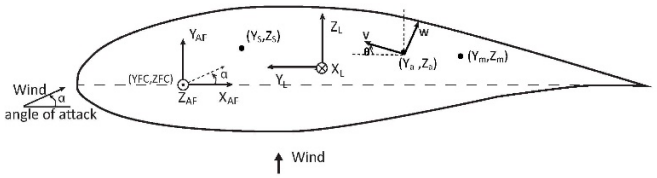

Figure 6 *:* Definition of foil (Y_{FC},Z_{FC}), area(Y_a,Z_a), shear (Y_s,Z_s) and mass centre (Y_m,Z_m) and inclination of foil system in the local cross section (strength) system (X_L,Y_L,Z_L)

In this paper it is assumed that the area centre of the beam is coincident with the Elastic centre (Y_L,Z_L) given in Figure 5, which is taken as the origin of the local coordinate system. With such an assumption, the coordinate of the Area centre is (0,0) in the local coordinate system (i.e. the local origin and area centre are coincident), see Figure 6.

For this study, the information about centres positions and angle θ as well as the stiffness properties are obtained from the DTU wind energy report-I-0092 [27]. Note that the orientation of the local coordinate system orientation set in RIFLEX matches with the one in [27].

Calibration of the double symmetric section type

This cross-section type is a simplification of the general cross section described previously and has been used in RIFLEX to model the blade originally. This cross section is easier to calibrate since the double symmetry assumption induces that the mass centre, area centre and shear centre are the same and coincident with the elastic reference centre illustrated in Figure 6. In addition, the angle θ is set to 0 and the stiffness properties are expressed in the local (X_L,Y_L,Z_L) coordinate system.

ABAQUS benchmark

The implementation of the generalised formulation was first checked against an equivalent ABAQUS model of the DTU 10MW blade, using the generalised beam formulation of ABAQUS [28] to compare the numerical results with the generalised beam formulation implemented in RIFLEX.

The blade consisted of 26 generalised beam elements with 26 cross sections. No pre-bent is applied during these preliminary checks, to keep the model as simple and representative as possible between the two solvers.

A representation of the blade in RIFLEX and ABAQUS is given in Figure 7. It should be noted that the RIFLEX model uses the foil geometry defined in the airfoil section to render the beam model, while ABAQUS reconstructs the beam profile as elliptic based upon the mechanical properties input, which explains why the geometry rendering is different between the two models.

Note that the ABAQUS model axis orientation (x,y,z) matches with the (X_L,Y_L,Z_L) of the RIFLEX model.

Three load cases are imposed to the blade during these checks:

- A +/-7m node tip displacement imposed in y-direction, the other DOF of the tip nodes being fixed. See orientation on the ABAQUS picture Figure 7
- A +7 m tip displacement imposed in z-direction, the other DOF of the tip nodes being fixed. See orientation on the ABAQUS picture Figure 7

The 7 m tip displacement corresponds to the average deflection experienced by the blade at a constant speed of 11m/s in operating conditions.

Both load cases will trigger axial force and bending moment along the blade. Overall, the results from RIFLEX are in good agreement with the ABAQUS model; see Figure 8, Figure 9, Figure 10 and Figure 11.

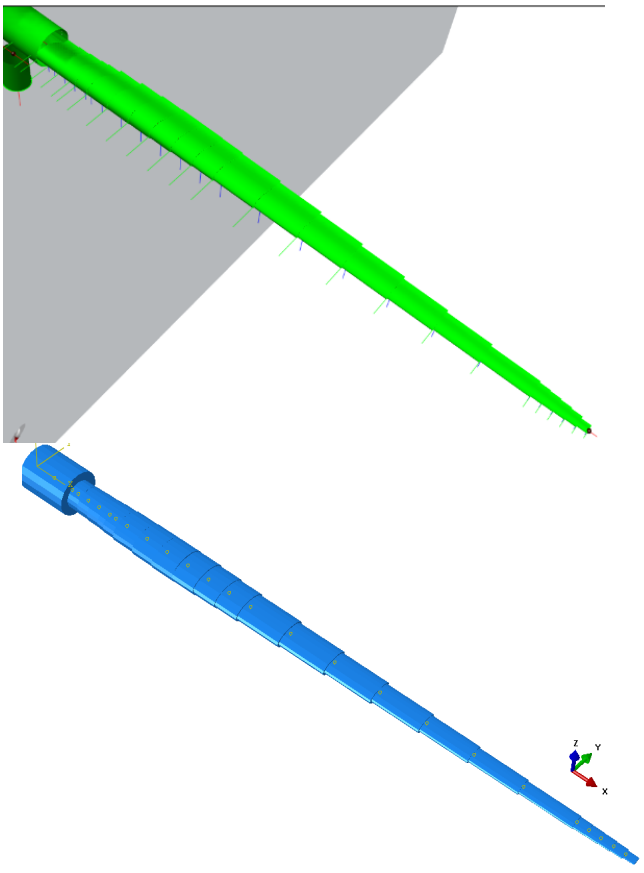

Figure 7 *:* RIFLEX (Up) and equivalent ABAQUS (Bottom) blade model used to check generalized beam formulations.

In particular, the responses obtained from the different displacement directions are well captured. If a displacement in y-direction is applied to the tip, the unsymmetrical shape of the blade with respect to the *xz-plane* will trigger a different mechanical response depending on the orientation of the displacement, as depicted in Figure 9. This is accounted for by the decoupling of the mass, area and shear centres in the cross section formulation. If the simplified beam version is used however, the y-displacement will trigger the same response in both orientation, due to the double symmetric assumption of the beam formulation. In the other hand, the symmetry of the blade with respect to *xy-plane* will lead to a similar behaviour between the two beam formulations if a z-displacement is applied, as depicted in Figure 10 and Figure 11.

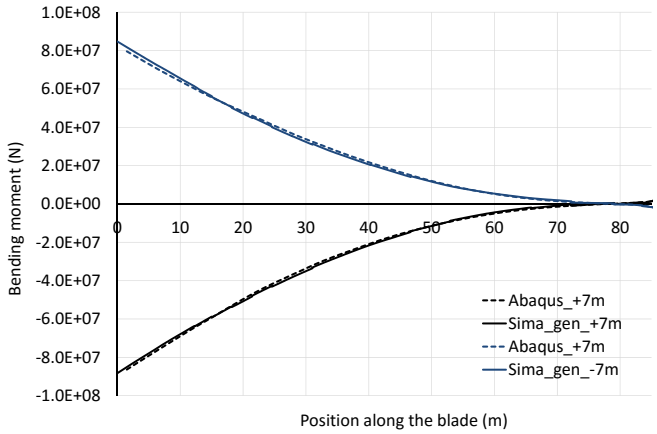

Figure 8 : Bending moment distribution along the blade, ABAQUS/RIFLEX comparison. +/-7m displacement of the tip node in y-direction.

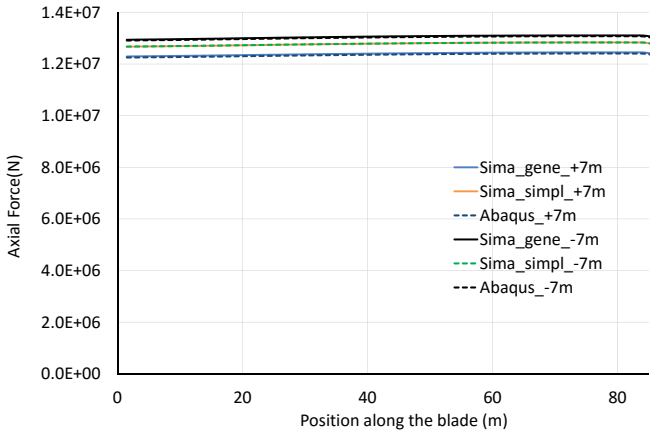

Figure 9 : Axial load distribution along the blade, ABAQUS/RIFLEX comparison. +/-7m displacement of the tip node in y-direction.

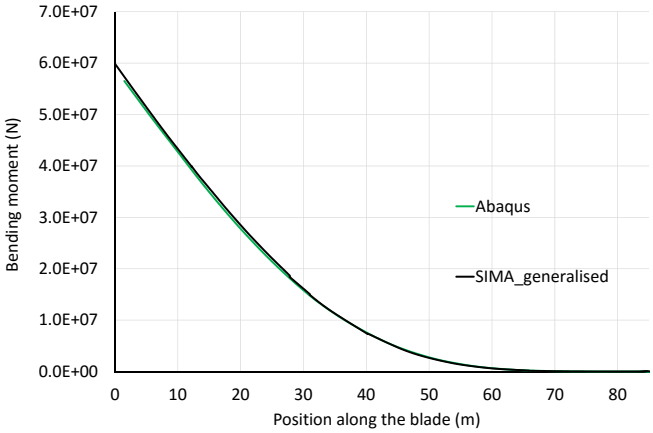

Figure 10 Bending moment distribution along the blade, ABAQUS/RIFLEX comparison. -7m displacement of the tip node in z-direction.

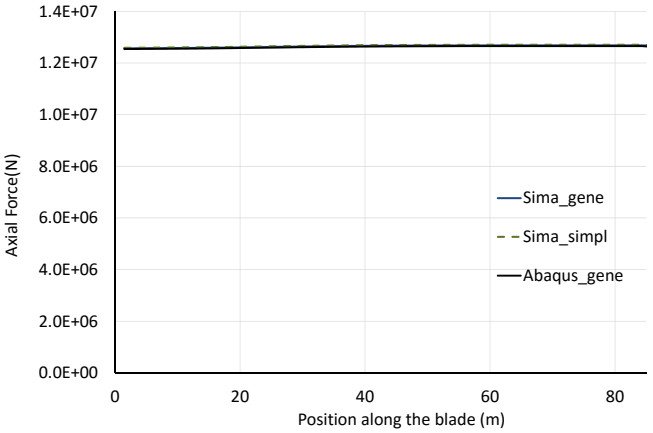

Figure 11 : Axial load distribution along the blade, ABAQUS/RIFLEX comparison. -7m displacement of the tip node in z-direction.

RESULTS WITH DTU 10MW WINDTURBINE

Three sets of results are presented in the following sections. Blade local values are expressed in the local coordinate system of the blade (X_L,Y_L,Z_L), defined in Figure 6.

- Effect at different constant wind speed and constant rotational speed, typically ranging from 8 to 24 m/s
- Effect at different yawed inflow at a constant wind speed (from 0 to 30°)
- Effect for a turbulent wind at rated 11 m/s wind speed

Constant wind speed, constant rotational speed

The local predicted loads in the blade and resultant thrust and torque were compared for several wind speed, respectively

below (8 m/s), at (11 m/s) and above (24 m/s) rated wind speed. Tower shadow effect is included.

There is a slight difference that can be observed at 8m/s and 24 m/s on the resulting values measured in the shaft, which is less noticeable at 11m/s, see Figure 12 and Figure 13. This can be correlated to the local data measured at the root of the blade, see Figure 14. At 8m/s and 24m/s, the bending moment is slightly lower for the generalised beam model than for the original beam model. This is explained by the anisotropic nature of the blade that can be captured with the generalised beam version but not with the original double symmetric one. It results in lower loads transmitted to the shaft.

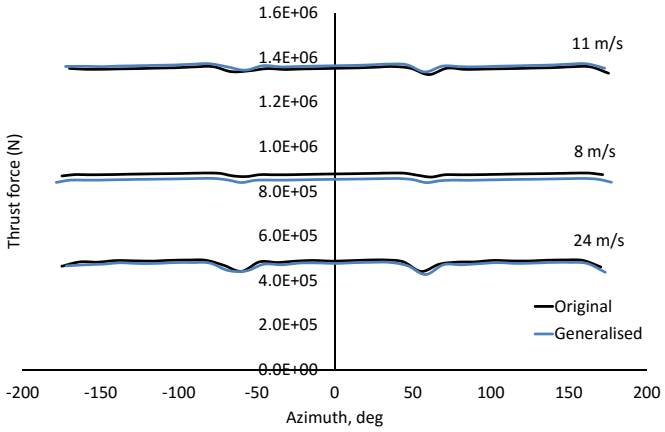

Figure 12 : Effect of the beam formulation on the resulting aero-force X in shaft for three wind speeds, as function of azimuth.

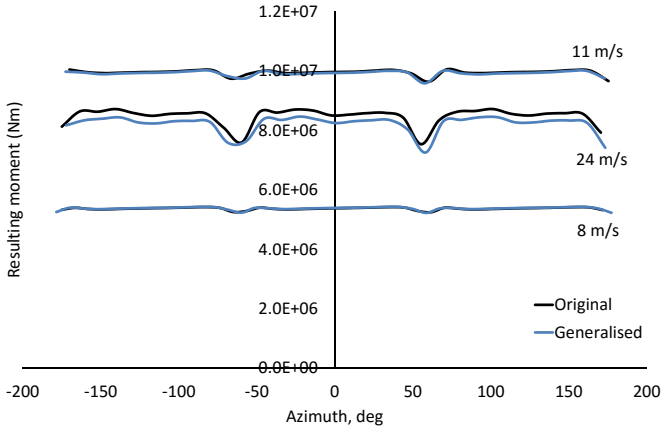

Figure 13 : Effect of the beam formulation on the resulting moment in shaft for three wind speeds, as function of azimuth.

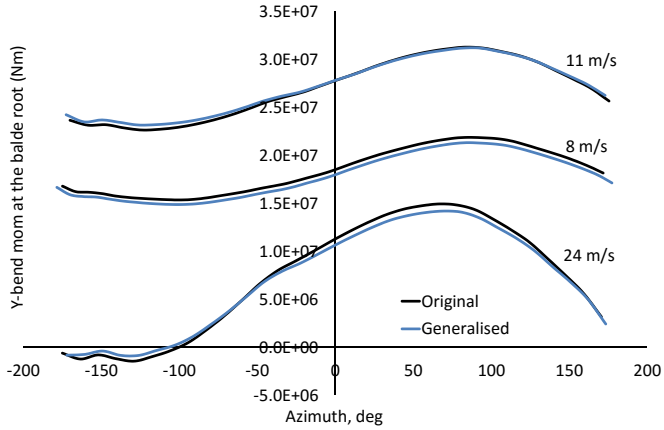

Figure 14 : Effect of the beam formulation on the bending moment at the blade root for three wind speeds, as function of azimuth.

Yawed inflow, constant wind speed

The local and resultant loads were compared for constant yawed inflow of 11 m/s at an angle of 15 and 30°. It should be noted that the accuracy of BEM for larger yaw angle is decreased. However, since the two beam formulations are compared at the same inflow, the results are still comparable. Figure 15 and Figure 16 show the azimuthal variation of the thrust and torque respectively while Figure 17 shows the azimuthal variation of the bending moment at the root of the blade for the different yawed inflow conditions.

The blade formulation has clearly an increased effect on the performances if the angle increases with a difference between the two models of approximately 6% at 30°-yawed inflow. This is correlated to the evolution of the blade properties at the blade root and to the control system, which actively compensates the change of mechanical properties between the two blades model by adapting the pitch angle. At 0° inflow, the pitch angle is 2.9° for the original blade model while it is 2.2° when using the generalised beam version. At 15° inflow, it is 1.7° while at 1.2° for the generalised version. At 30° inflow however the pitch angle remains at 1.2° for both beam formulations, and the anisotropic properties of the blade result in different bending moment at the blade root, see Figure 17, and subsequently to a noticeable variation of the thrust force and resulting torque in shaft, see Figure 15 and Figure 16.

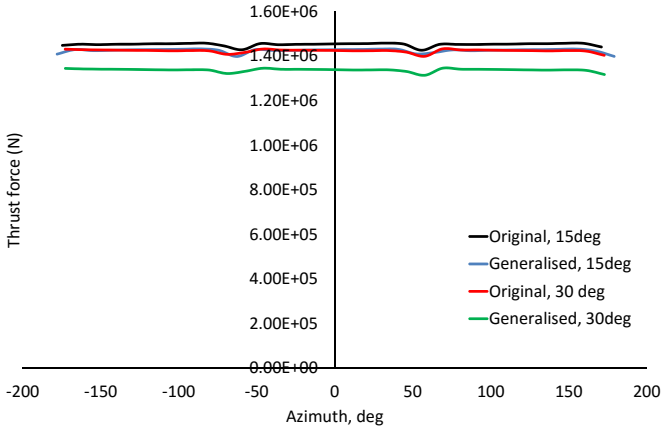

Figure 15 : Effect of the beam formulation on the resulting thrust force in shaft for two inflow angles, as function of azimuth.

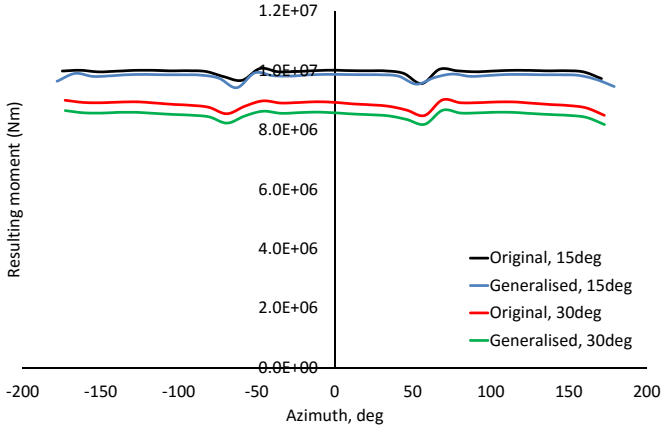

Figure 16 : Effect of the beam formulation on the resulting moment in shaft for two inflow angles, as function of azimuth.

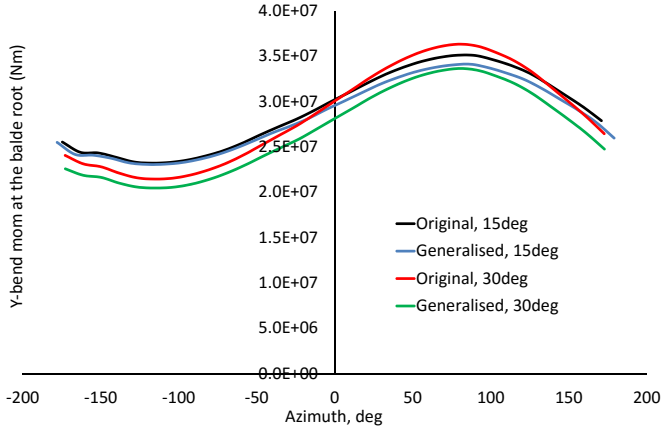

Figure 17 : Effect of the beam formulation on the bending moment at the blade root for two inflow angles, as a function of the azimuth

Turbulent wind, constant rotational speed

Finally, the local and global response in turbulent wind were examined for constant rotational speed (9.6 RPM). The mean wind speed was 12 m/s, and the turbulence intensity was 10.6 % (at the hub height), see Figure 18. Short portions of the time series of the wind velocity and selected local and global loads are shown in Figure 19, Figure 20 and Figure 21, respectively. As shown, the results are similar for a large portion of the time series except for short period between 250-280s and 350-400s, which can be explained by the dynamic pitch evolution during these two short periods, which slightly differs between the two models.

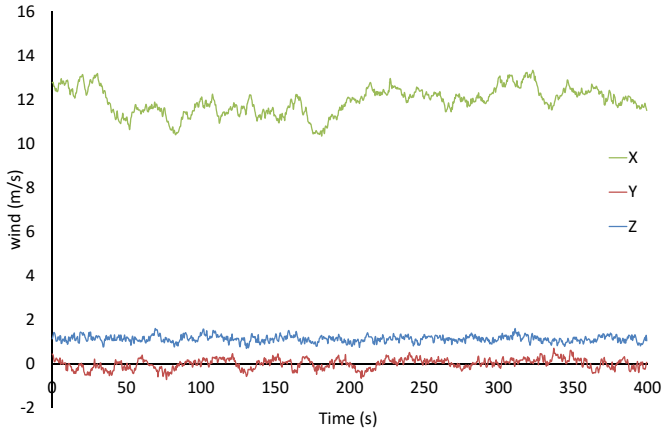

Figure 18 : Turbulent wind velocity at the hub.

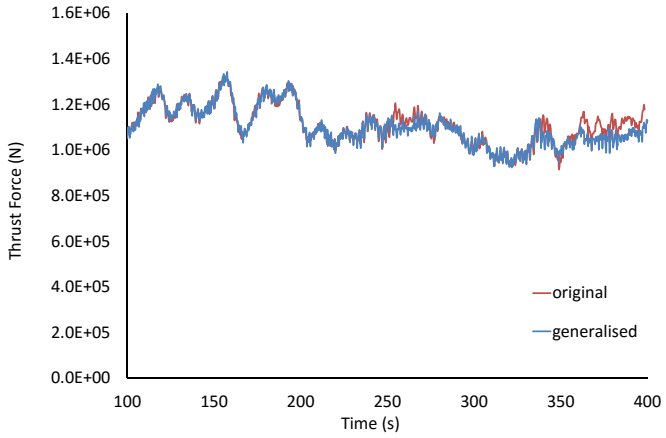

Figure 19 : effect of the beam formulation on the time varying thrust load, constant rotor speed (9.6rpm), mean wind speed 12m/s.

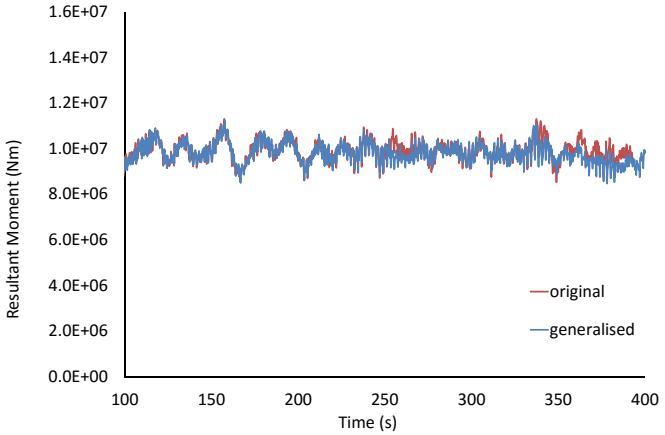

Figure 20 : : effect of the beam formulation on the time varying resulting moment, constant rotor speed (9.6rpm), mean wind speed 12m/s.

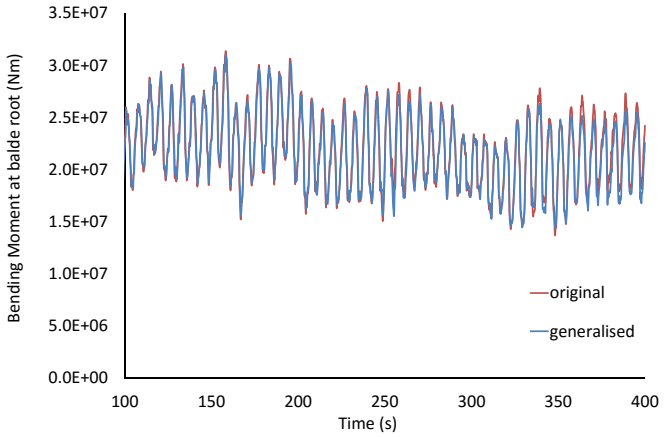

Figure 21 : effect of the beam formulation on the time varying local bending moment at the blade root, constant rotor speed (9.6rpm), mean wind speed 12m/s.

Results summary

The following tables summarize the different results obtained from the calculations of the different load cases investigated. The mean value and standard deviation of the stationary part of the signals are used for comparison. Overall, the difference between the two formulations remains low in terms of mean values (5% at max) and standard deviation (up to 10% on the local bending moment for an inflow angle of 30°). In most of load cases, the use of generalised formulation leads to a slight decrease of the reported values.

Table 2 : Results comparison on the mean value and standard deviation of the thrust force measured in shaft for the two blade formulations under various constant wind speeds and inflow angles.

		Thrust force (N)					
wind speed	direction	original		Generalized			
		mean	dev.	mean	diff(%)	dev.	diff(%)
8m/s	0°	8.76E+05	4.5E+03	8.54E+05	**-2.53**	4.5E+03	**-0.89**
	15°	8.71E+05	4.1E+03	8.47E+05	**-2.85**	4.0E+03	**-2.54**
	30°	8.04E+05	3.6E+03	7.77E+05	**-3.33**	3.6E+03	**0.64**
11m/s	0°	1.35E+06	8.2E+03	1.35E+06	**-0.04**	8.0E+03	**-1.76**
	15°	1.45E+06	8.0E+03	1.43E+06	**-1.47**	8.0E+03	**-0.83**
	30°	1.42E+06	7.5E+03	1.34E+06	**-5.74**	7.3E+03	**-2.60**
24m/s	0°	4.79E+05	1.4E+04	4.68E+05	**-2.20**	1.4E+04	**0.70**
	15°	4.56E+05	1.4E+04	4.55E+05	**-0.39**	1.4E+04	**-1.40**
	30°	3.51E+05	1.5E+04	3.51E+05	**0.04**	1.6E+04	**1.30**

Table 3 : Results comparison on the mean value and standard deviation of the resulting torque measured in shaft for the two blade formulations under various constant wind speeds and inflow angles.

		Resulting torque (Nm)					
wind speed	direction	original		Generalized			
		mean	dev.	mean	diff(%)	dev.	diff(%)
8m/s	0°	5.36E+06	4.7E+04	5.36E+06	**0.07**	4.6E+04	**-2.11**
	15°	5.33E+06	5.4E+04	5.31E+06	**-0.34**	5.2E+04	**-4.07**
	30°	4.91E+06	6.2E+04	4.85E+06	**-1.19**	6.0E+04	**-3.40**
11m/s	0°	9.94E+06	9.8E+04	9.88E+06	**-0.58**	9.4E+04	**-3.58**
	15°	9.93E+06	1.2E+05	9.81E+06	**-1.21**	1.1E+05	**-3.42**
	30°	8.84E+06	1.3E+05	8.52E+06	**-3.52**	1.2E+05	**-8.96**
24m/s	0°	8.43E+06	3.1E+05	8.19E+06	**-2.80**	3.1E+05	**-0.64**
	15°	8.08E+06	4.0E+05	8.03E+06	**-0.60**	4.0E+05	**-1.24**
	30°	7.11E+06	3.9E+05	7.08E+06	**-0.44**	3.7E+05	**-3.36**

Table 4 : Results comparison on the mean value and standard deviation of the bending moment measured at the blade root for the two blade formulations under various constant wind speeds and inflow angles.

		Bending moment (Nm)					
wind speed	direction	original		Generalized			
		mean	dev.	mean	diff(%)	dev.	diff(%)
8m/s	0°	1.84E+07	2.3E+06	1.80E+07	**-2.46**	2.3E+06	**-0.43**
	15°	1.82E+07	3.1E+06	1.77E+07	**-3.00**	3.0E+06	**-4.50**
	30°	1.67E+07	3.5E+06	1.65E+07	**-1.17**	3.4E+06	**-3.72**
11m/s	0°	2.70E+07	3.0E+06	2.68E+07	**-0.70**	2.9E+06	**-5.26**
	15°	2.90E+07	4.2E+06	2.85E+07	**-1.80**	4.0E+06	**-6.40**
	30°	2.84E+07	5.2E+06	2.67E+07	**-5.72**	4.7E+06	**-10.50**
24m/s	0°	7.11E+06	5.9E+06	6.93E+06	**-2.53**	5.5E+06	**-6.83**
	15°	6.80E+06	2.0E+06	6.76E+06	**-0.58**	2.2E+06	**8.54**
	30°	5.40E+06	4.5E+06	5.32E+06	**-1.51**	4.4E+06	**-2.67**

CONCLUSIONS

The effect of a general beam formulation with eccentric shear and mass centres used to discretize the blades of the 10MW reference wind turbine was presented in this paper and compared to the simplified double symmetric cross section generally used in RIFLEX.

A slight retardation of the signals is observed, as well as a slight amplitude difference. This difference remains very low however (5-6% at max on mean values, and up to 10% in terms of standard deviation) and increases with yawed inflow angle.

The retardation of the signals is typically due to the accounting of the eccentric mass in the beam formulation, which triggers a phase difference with the original formulation as the inertial properties of the blade system are modified.

This effect is even more noticeable during the initial transitional phase of the simulation (Not represented here, only the stationary phase is represented), where inertial effects are more predominant.

In all the cases investigated, it was found that the beam formulation has limited effect on the resulting local forces. This is explained by the blade technology used today: the torsional moments applied to the blade remain very small in operations due to the active pitch angle control systems. However, such a formulation could have higher effects on the next generation twisting blades, where increased moments will be expected during operations.

It would be interesting as further work to run a benchmark comparison between RIFLEX and HAWC2 (2015, [29]) using new beam capabilities between the two codes to analyse the next-gen blades where bending-twist effect are more important.

ACKNOWLEDGMENTS

This work has been carried out as part of NOWITECH (Norwegian Research Centre for Offshore Wind Technology) which is co-funded by the Research Council of Norway, industrial companies and participating research organizations (http://www.nowitech.no).

REFERENCES

1. Kooijman HJT (1996). Bending-torsion coupling of a wind turbine rotor blades. ECN-I-96-060, *Netherlands Energy Research Foundation*.
2. Hodges, D.H., Atilgan, A.R., Cesnik, C.E.S., Fulton, M.V. (1999). On a Simplified Strain Energy Function for Geometrically Nonlinear Behaviour of Anisotropic Beams. *Composites Engineering*, Vol. 2, No. 5-7, 1992, pp. 513-526.
3. Yu W, Hodges DH, Volovoi VV, Cesnik CES (2002). On Timoshenko-Like Modeling of Initially Curved and Twisted Composite Beams. *International Journal of Solids and Structures*, Vol. 39, No. 19, pp. 5101-5121.
4. Berdichevsky VL (1979). Variational-Asymptotic Method of Constructing a Theory of Shells. *PMM*, Vol. 43, No. 4, 1979, pp. 664-687.
5. Otero, A.D., Ponta, F.L. (2010). Structural Analysis of Wind-Turbine Blades by a Generalized Timoshenko Beam Model. *Journal of Solar Energy Engineering,*
6. Branner, K. et al.(2012). Anisotropic beam model for analysis and design of passive controlled wind turbine blades. *DTU E-report*.
7. Kim, T., Hansen, A. M., & Branner, K. (2013). Development of an anisotropic beam finite element for composite wind turbine blades in multibody system. *Renewable Energy*, 59, 172-183.
8. Lobitz DW, Veers PS, Laino DJ (2000). Performance of twist-coupled blades on variable speed rotors. *Proceedings of the 2000 ASME Wind Energy Symposium*, Reno, NV, 404-412.
9. Lobitz DW, Veers PS. (2003). Load Mitigation with Bending/Twist-coupled Bladeson Rotors Using Modern Control Strategies. *Wind Energy* 6: 105-117.
10. MARINTEK (2015). RIFLEX 4.9.0 User's Manual. Norway: MARINTEK.
11. MARINTEK (2015). RIFLEX 4.9.0 Theory Manual. Norway: MARINTEK.
12. Ormberg, H., Passano, E., & Luxcey, N. (2011, January). Global Analysis of a Floating Wind Turbine Using an Aero-Hydro-Elastic Model: Part 1—Code Development and Case

Study. *ASME 2011 30th International Conference on Ocean, Offshore and Arctic Engineering*, ASME, pp. 837-847.
13. Ormberg, H., Fylling, I., Larsen, K., & Sødahl, N. (1997). Coupled analysis of vessels motions and mooring and riser system dynamics. *Proc. ASME 1997 16th International Conference on Offshore Mechanics and Arctic Engineering*. Yokohama, Japan, ASME, 91-100.
14. Kendon, T. E., Oritsland, O., Baarholm, R. J., Karlsen, S. I., Stansberg, C.-T., Rossi, R. R., Barreira, Rodrigo A, Matos, V. L. F., Sales, J. S. (2008). Ultra-deepwater model testing of a semisubmersible and hybrid verification. *Proc ASME 2008 27th International Conference on Offshore Mechanics and Arctic Engineering*. Estoril, Portugal, American Society of Mechanical Engineers, 277-290.
15. Ormberg, H., Stansberg, C. T., Yttervik, R., & Kleiven, G. (1999). Integrated vessel motion and mooring analysis applied in hybrid model testing. *Proc. 22nd International Ocean and Polar Engineering Conference*, Brest, France, ISOPE, 1, 339-346.
16. Stansberg, C. T., Yttervik, R., Øritsland, O., & Kleiven, G. (2000). Hydrodynamic model test verification of a floating platform system in 3000m water depth. *Offshore Technology Conference*, Houston, TX, USA, OTC, 1, 1, 1-9.
17. Stansberg, C. T., Øritsland, O., & Kleiven, G. (2000). Reliable methods for verification of mooring and station keeping in deep water. *Proc. Offshore Mechanics and Arctic Engineering Conference,* New Orleans, USA, ASME.
18. Bak, C., Zahle, F., Bitsche, R., Kim, T., Yde, A., Henriksen, L. C., Andersen, P.B. Natarajan, A., Hansen, M. H.. Design and performance of a 10 MW wind turbine. *Journal of Wind Energy*. (2014).
19. Burton, T., Jenkins, N., Sharpe, D., & Bossanyi, E. (2011). *Wind Energy Handbook*: Wiley.
20. Hansen, M. O. L., Sørensen, J. N., Voutsinas, S., Sørensen, N., & Madsen, H. A. (2006). State of the art in wind turbine aerodynamics and aeroelasticity. *Progress in Aerospace Sciences,* 42(4), 285-330.
21. Manwell, J. F., McGowan, J. G., & Rogers, A. L. (2009). *Wind Energy Explained*: John Wiley & Sons, Ltd.
22. Moriarty, P. J., & Hansen, A. C. (2005). AeroDyn Theory Manual.
23. Battini, J. M., & Pacoste, C. (2006). On the choice of the linear element for corotational triangular shells. Computer methods in applied mechanics and engineering, 195(44), 6362-6377.
24. Felippa, C. A. and Haugen, B. (2005): A unified formulation of small-strain corotational finite elements: I.Theory. *Computer Methods in Applied Mechanics and Engineering*, Vol. 194, pp. 2285-2335, 2005.
25. Mathisen, K. M. (1990): Large displacement analysis of flexible and rigid systems considering displacement dependent loads and nonlinear constraints. *PhD thesis, Department of Structural Engineering, The Norwegian Institute of Technology, Trondheim, Norway.*
26. *Bell, K. [1987]: Matrisestatikk. Tapir Forlag, Trondheim, Norway.*
27. Christian Bak, Frederik Zahle, Robert Bitsche, Taeseong Kim, Anders Yde, Lars Christian Henriksen, Anand Natarajan, *Morten Hartvig Hansen.* Description of the DTU 10 MW Reference Wind Turbine. *DTU Wind Energy Report-I-0092.* July 2013.
28. SIMULIA *ABAQUS 6.14 ANALYSIS USER'S GUIDE VOLUME IV: ELEMENTS. Dassault systems.*
29. Torben, J.L., Anders M.H. (2015). *How 2 HAWC2, the user's manual V4.6.*